linear optics. The distinctively chemical perspective from which MVS has evolved places it in a rather unique position to prepare new "nanocrystalline" and "nanophase" composites[79] that are currently under examination in a number of laboratories. Future work would do well to link MVS as a specialized materials methodology to timely and well-conceived applications in these areas. Although more research is needed to develop the full scientific and technological potential of MVS in polymer science, the results of the research reported to date should continue to stimulate activity in this area.

(79) Eastman, J.; Siegel, R. W. *Res. Dev.* **1988**, *Jan*, 56.

Articles

High-Resolution Electron Microscopy and Image Simulation of TT-, T-, and H-Niobia and Model Silica-Supported Niobium Surface Oxides

J. G. Weissman,[†,§] E. I. Ko,[*,†] P. Wynblatt,[‡] and J. M. Howe[‡]

Department of Chemical Engineering and Department of Metallurgical Engineering and Materials Science, Carnegie Mellon University, Pittsburgh, Pennsylvania 15213

Received June 27, 1988

The behavior of silica-supported niobium surface oxides during heat treatment was examined by high-resolution transmission electron microscopy (HRTEM). Surface oxides, consisting of between 4 and 50 Å Nb_2O_5 reactively radio-frequency sputter deposited onto 800 Å SiO_2, were calcined at 773 and 873 K for up to 16 h and were so designed to approximate high-surface-area materials suitable for catalytic applications. Also examined was the stability of three known crystalline forms of niobia, TT-, T-, and H-Nb_2O_5. Lattice image simulations were necessary to unequivocally identify the various Nb_2O_5 phases observed. TT- and T-Nb_2O_5 were found to have a nearly identical structure; a structure for TT-Nb_2O_5 is proposed. Besides amorphous monolayers, two major types of crystalline Nb_2O_5 were found on the surface oxide samples: very small crystals corresponding to T-Nb_2O_5, which could not be unambiguously defined by HRTEM in terms of thickness or orientation, and relatively large crystals of H-Nb_2O_5. These findings are discussed in terms of literature results, and a new model for the phase-transition behavior of Nb_2O_5 is presented.

Introduction

One class of industrially important catalytic systems is that of surface oxides, in which one oxide is supported on the surface of a different high-surface-area oxide; their uses include oxidation of olefins and production of unsaturated hydrocarbons.[1,2] The surface oxide can be dispersed over the support in amorphous monolayer or multilayer coverages, or as distinct crystallites, or a combination of these types, depending on the strength of interfacial interaction between the support and the supported oxides and the loading of the surface oxide. There has been an increasing body of evidence (for example, ref 3–6) that points to the importance of such an interaction on the structural and chemical properties of these systems. Our program of studying the catalytic and physical properties of surface oxides has recently led to the preparation of thin films consisting of niobium surface oxides supported on silica (Nb_2O_5–SiO_2), characterized by surface analysis and conventional electron microscopy (TEM).[7,8] The films were prepared in such a way as to mimic their high-surface-area counterparts,[9] so as to obtain structural information on this system.

Our previous results showed that there are important differences between the thin-film and high-surface-area samples toward calcining. Three types of Nb_2O_5 were found to occur on the thin-film samples: I, niobia strongly held to the surface via direct niobium–oxygen–silicon bonds; II, niobia crystallizing under the influence of the surface; III, niobia not interacting with the surface. Types I and II were also found to occur on the high-surface-area samples. Reasons for the appearances of the different types of niobia on different samples are discussed elsewhere and depend on a combination of factors including surface hydroxyl concentration of the silica substrate and reactivity of the Nb_2O_5 precursor.[8,10]

Since the structure of a supported oxide, in this case niobia, is important in understanding its reactivity as well

* To whom correspondence should be sent.
† Department of Chemical Engineering.
‡ Department of Metallurgical Engineering and Materials Science.
§ Present address: Texaco, Inc., P.O. Box 509, Beacon, NY 12508.

(1) Haber, J. *ACS Symp. Ser.* **1985**, *279*, 3.
(2) Courtine, P. *ACS Symp. Ser.* **1985**, *279*, 37.
(3) Nag, N. K. *J. Phys. Chem.* **1987**, *91*, 2324.
(4) Kijenski, J.; Baiker, A.; Glinski, M.; Dollenmeier, P.; Wokaun, A. *J. Catal.* **1986**, *101*, 1.
(5) Hayden, T. F.; Dumesic, J. A.; Sherwood, R. D.; Baker, R. T. K. *J. Catal.* **1987**, *105*, 299.
(6) Reichmann, M. G.; Bell, A. T. *Langmuir* **1987**, *3*, 111.
(7) Weissman, J. G.; Ko, E. I.; Wynblatt, P. *J. Vac. Sci. Technol. Part A* **1987**, *5*, 1694.
(8) Weissman, J. G.; Ko, E. I.; Wynblatt, P. *J. Catal.* **1987**, *108*, 383.
(9) Ko, E. I.; Bafrali, R.; Nuhfer, N. T.; Wagner, N. J. *J. Catal.* **1985**, *95*, 260.
(10) Weissman, J. G. Ph.D. Thesis, Carnegie Mellon University, 1987.

0897-4756/89/2801-0187$01.50/0

as its interaction with the substrate, we undertook a high-resolution transmission electron microscopy (HRTEM) study aimed at positively identifying the various niobia forms previously observed on our thin-film samples with conventional TEM. To supplement these observations, several pure niobia forms were synthesized in our laboratory and observed by HRTEM. The images obtained were interpreted with optical diffraction and image simulation, using the simulated high-resolution lattice image (SHRLI) programming package.[11]

Before presenting the results, we would like to describe briefly the various structural forms of niobia. According to the nomenclature of Shafer et al.,[12] niobia exists as TT-, T-, B-, N-, P-, M-, and H-Nb_2O_5. Many of these forms are metastable under normal conditions, and some of them are structurally quite similar. Our focus will be on TT- and T- (two low-temperature forms) and H-Nb_2O_5 (a high-temperature form), as they are prevalent in our samples.

The behavior of niobia is well understood at pressures above 300 MPa, but reliable low-pressure, low-temperature studies on niobia are lacking. There remain some controversies over which form is stable over which temperature region.[13-18] Another complication is that many results were obtained by using niobia precursor compounds containing chloride ions, such as $NbOCl_3$, HCl, or Cl_2, either as starting materials or transport agents.[12,15,16,19,20] Chloride and other impurities have been found to greatly increase the stability of metastable niobia forms, such as P- or M-Nb_2O_5 and most likely B-Nb_2O_5 as well.[10,12]

We will show that by using a precursor that was free of impurities, it was possible to stabilize H-Nb_2O_5 at temperatures lower than what has been reported. Furthermore, new information on the structures of TT- and T-Nb_2O_5 has been obtained in this study. Our observations on pure niobia further provided the groundwork for understanding supported niobia in the thin-film samples, and together these results led to a model for the stability of the various niobia forms.

Experimental Procedures

Sample Preparation. Methods for preparing niobia on silica thin films have been discussed elsewhere.[8,10] Approximately 800-Å-thick SiO_2 films were prepared by first evaporating silicon onto NaCl crystal cleavage fragments inside a 1.3×10^{-5} Pa vacuum. The salt was removed by dissolution in water; the released flakes of silicon were picked up onto stainless steel TEM grids. These were then oxidized at 1273 K for 4 h, producing a homogeneous, nearly amorphous SiO_2 substrate. Niobia was deposited by radio-frequency sputtering inside a chamber held at 6 Pa of an argon–oxygen mixture, resulting in reactively sputtered films close to Nb_2O_5 in composition. The films were fully oxidized to Nb_2O_5 after exposure to atmosphere.

Following sputtering, the films were calcined at either 773 or 873 K, from 2 to 16 h, in an O_2/N_2 air mixture (Airco, dry) at 10 L/min. These conditions are similar to those used to calcine the high-surface-area samples.[9] The samples were first examined by TEM, as reported earlier,[8] and then by HRTEM. The nomenclature describing these samples is as follows: a sample containing an equivalent thickness of 4 Å Nb_2O_5, calcined at 873 K for 2 h is labeled 4(873,2).

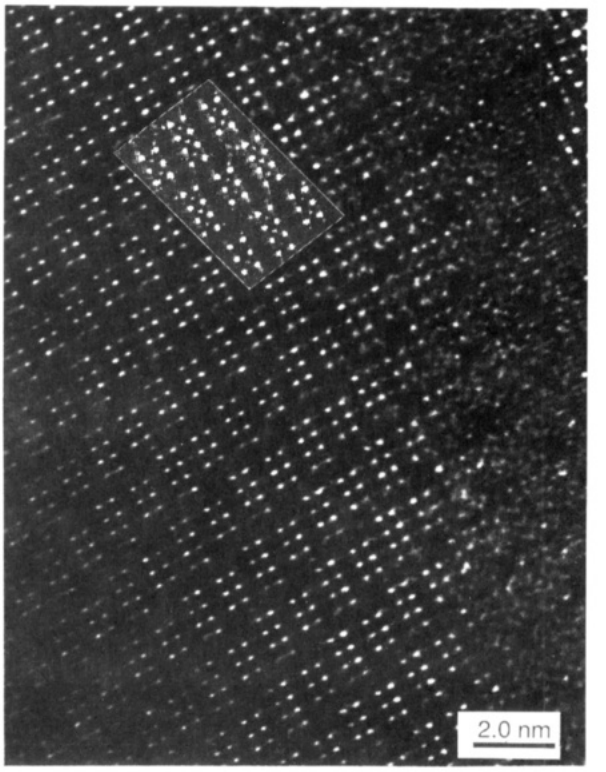

Figure 1. HRTEM and image simulation for H-Nb_2O_5(010). Image simulated at slice 50- and 96-Å thickness, −250-Å defocus.

TT-, T-, and H-Nb_2O_5 were prepared by precipitating Nb_2O_5 from a hexane solution of niobium(V) ethoxide with ammonium hydroxide and then calcined under the appropriate conditions to yield the desired form.[12] Powder X-ray diffraction (XRD) patterns of these samples were identical with those in the literature.[21-23] The pure forms were examined by HRTEM with the goal of using their images to confirm reported structures by image simulation.

High-Resolution Electron Microscopy and Image Simulation. High-resolution electron microscopy was performed on a JEOL 4000EX at the Center for Solid State Science at Arizona State University. The microscope was operated at 400 keV accelerating potential and had an interpretable point resolution of 1.8 Å, which permitted direct observation of crystal structures. Most images were obtained at a magnification of 600 000 times, corrected afterward through calibration of the known variations in the objective lens current. Images were obtained at the thin specimen edge near optimum (Scherzer) defocus, which facilitates direct interpretation of the image in terms of the crystal structure.[24]

High-resolution image simulations were performed by using the SHRLI computer programs described by O'Keefe et al.[11] These programs require input of the crystal space group and atom positions within the unit cell and utilize the multislice method to calculate the scattered amplitudes for a specific crystal thickness. Essentially, the process consists of dividing a crystal to be simulated into thin slices of equal thickness and following the electron wave function as it propagates through each slice to yield the resulting wave function at the exit surface of the crystal. The exit amplitude is further modified by microscope parameters[10] such as lens aberrations and beam convergence, which are also included in the calculations, and the resulting magnified image

(11) O'Keefe, M. A.; Buseck, P. R. *Trans. Am. Cryst. Assoc.* **1979**, *15*, 27.
(12) Schafer, H.; Gruehn, R.; Schulte, F. *Ang. Chem., Internat. Ed. Engl.* **1966**, *5*, 40.
(13) Tamura, S. *J. Mater. Sci.* **1972**, *7*, 298.
(14) Waring, J. L.; Roth, R. S.; Parker, H. S. *J. Res. Natl. Bur. Stand. Sect. A* **1973**, *77A*, 705.
(15) Hibst, H.; Gruehn, R. *Z. Anorg. Allg. Chem.* **1978**, *440*, 137.
(16) Izumi, F.; Kodama, H. *Z. Anorg. Allg. Chem.* **1978**, *440*, 155.
(17) Kodama, H.; Goto, M. *Z. Anorg. Allg. Chem.* **1976**, *421*, 71.
(18) Tamura, S.; Kato, K.; Goto, M. *Z. Anorg. Allg. Chem.* **1974**, *410*, 313.
(19) Ritschel, M.; Oppermann, H.; Mattern, N. *Krist. Tech.* **1978**, *18*, 1421.
(20) Kodama, H.; Kikuchi, T.; Goto, M. *J. Less-Common Metals* **1972**, *29*, 415.
(21) Burke, P. A., private communication.
(22) Holtzberg, F.; Reisman, A.; Berry, M.; Berkenbilt, M. *J. Am. Chem. Soc.* **1957**, *79*, 2039.
(23) Powder Diffraction File Numbers 7-61 and 27-1003, JCPDS International Centre for Diffraction Data.
(24) Spence, J. C. H. *Experimental High-Resolution Electron Microscopy*, Clarendon Press: Oxford, 1981; pp 85, 102, 135.

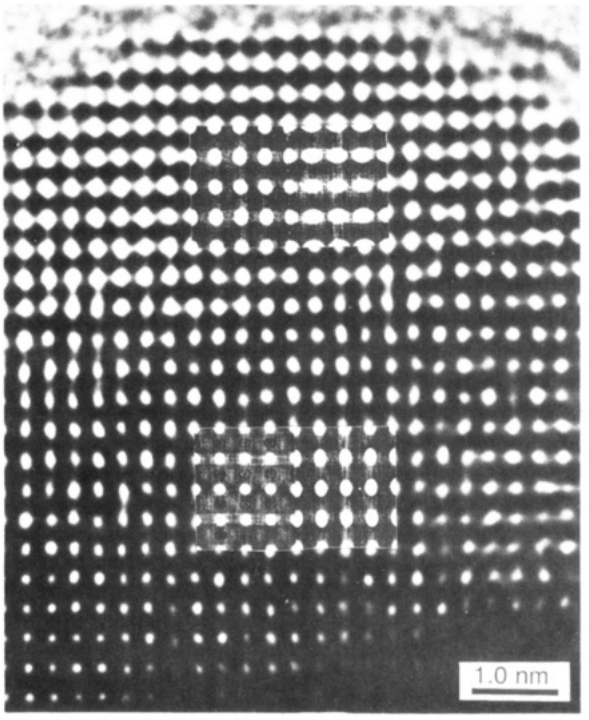

Figure 2. HRTEM of TT-Nb_2O_5(001) and corresponding image simulations with use of TT-Nb_2O_5(001) and T-Nb_2O_5($\bar{8}10$) for a wedge-shaped crystal, with thinner region at the top of the figure. Images on left simulated with the T-Nb_2O_5 structure and images on right simulated with the TT-Nb_2O_5 structure, described in the text. For both sides, the top images are at slice 25 and the bottom images at slice 50, corresponding to 50- and 100-Å thickness, all at −460-Å defocus.

is outputted to a laser writer emulating a line printer. A range of specimen thicknesses, defocus values, and in some cases crystallographic orientations was simulated until a suitable match with the experimental image was obtained. Lattice parameters, atomic coordinates, and thermal parameters for T-, B-, M-, N-, and H-Nb_2O_5 were obtained from the literature.[13,25-29]

Results and Discussion

Pure Niobia Phases. TT-, T-, and H-Nb_2O_5 were imaged by HRTEM, and examples of the results are given in Figures 1 and 2. The selected area electron diffraction patterns (SADP) and experimental structures for T- and H-Nb_2O_5 corresponded exactly to what we expected from the literature values. In fact, the calculated image in Figure 1 for H-Nb_2O_5(010) is an excellent fit, confirming the complex block structure of H-Nb_2O_5 calculated by single-crystal X-ray diffraction work.[29] The observed images of TT-Nb_2O_5 and T-Nb_2O_5 were similar, indicating that the two forms may either be identical or have very similar atomic structures. An electron diffraction pattern taken from the region shown in Figure 2 of TT-Nb_2O_5 can be indexed as either TT-Nb_2O_5(001) or T-Nb_2O_5($\bar{8}10$), as listed in Table I.

We first interpreted these results in terms of the arguments of Shafer et al.,[12] who considered the TT form to be a less crystalline case of T-Nb_2O_5 on the basis of XRD data. Our HRTEM images of TT-Nb_2O_5 appeared well-ordered and had no additional defects than were found in similar images of T-Nb_2O_5. From direct imaging we concluded that TT-Nb_2O_5 was not a less crystalline precursor of T-Nb_2O_5.

Table I. Indexing of Diffraction Pattern in Figure 2 to either TT-Nb_2O_5(001) or T-Nb_2O_5($\bar{8}10$)[a]

obsd	TT	T
3.94	3.94 (040)	3.93 (001)
3.14	3.16 (200)	3.14 ($\bar{1}80$)
2.46	2.46 (240)	2.45 ($\bar{1}81$)
1.97	1.96 (080)	1.97 (002)
1.56	1.58 (400)	1.57 ($\bar{2}$·16·0)
1.30	1.31 (0·12·0)	1.31 (003)

[a] *d* spacings are in angstroms, *hkl* indices enclosed in parentheses.

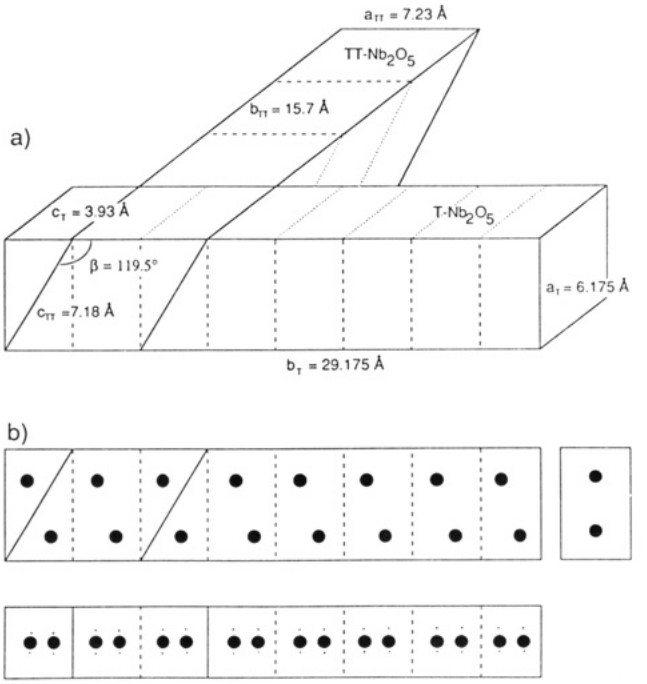

Figure 3. (a) Geometrical relationship between the unit cells of TT- and T-Nb_2O_5 as described in ref 13 and 25 and based on ref 30. Subscripts on the unit-cell dimensions refer to the particular form. Lattice vectors between the two cells related nearly by $^1/_2\bar{a}_{TT} = \bar{a}_T + {}^1/_8\bar{b}_T$, $\bar{b}_{TT} = 4\bar{c}_T$, $\bar{c}_{TT} = \bar{a}_T$; unit-cell dimensions, as indicated in the figure, nearly related by $a_{TT} = {}^1/_4 b_T$, $b_{TT} = 4c_T$, $c_{TT} = (a_T{}^2 + ({}^1/_8 b_T)^2)^{1/2}$, and $\beta = \tan^{-1}({}^1/_8 b_T/a_T) + 90°$. (b) Approximate projections of niobium atom positions in the T-Nb_2O_5 unit cell onto the *a*–*b* (left top), *a*–*c* (right), and *b*–*c* (bottom) crystal planes. In the lowermost panel, the larger dots represent the average niobium atom position, while the small dots represent the 32 8(*i*) half-occupancy positions of Nb in T-Nb_2O_5. As described in the text, Nb can occupy either one or the other of these positions. (Note that the relative displacement is exaggerated in the figure.) However, in TT-Nb_2O_5, Nb can occupy any position between the two smaller dots, while having an average position centered on the larger dot.

Figure 2 gives simulated images (shown on left) calculated with the structure of T-Nb_2O_5, at two thicknesses, superimposed on a wedge-shaped TT-Nb_2O_5 crystal, producing a satisfactory match. The atomic positions of TT- and T-Nb_2O_5 must be similar for the calculated image of one to fit the experimental image of the other. Yet X-ray diffraction data for the two forms result in indexing to different crystal groups (TT-Nb_2O_5 is monoclinic,[13] with a = 7.23, b = 15.7, c = 7.18 Å, β = 119.5°; T-Nb_2O_5 is orthorhombic, space group *Pbam*,[25] with a = 6.175, b = 29.175, c = 3.93 Å). There is no report on the structure of TT-Nb_2O_5 in the literature, but there are sufficient data from this work and from the literature to make a reasonable estimate.

(25) Kato, K.; Tamura, S. *Acta Crystallogr.* **1975**, *B31*, 673.
(26) Laves, F.; Petter, W.; Wulf, H. *Naturwiss* **1964**, *51*, 633.
(27) Mertin, W.; Andersson, S.; Gruehn, R. *J. Solid State Chem.* **1970**, *1*, 419.
(28) Andersson, S. *Z. Anorg. Allg. Chem.* **1967**, *351*, 106.
(29) Kato, K. *Acta Crystallogr.* **1976**, *B32*, 764.
(30) Terao, N. *Jpn. J. Appl Phys.* **1965**, *4*, 8.

Table II. Niobium Atom Positions for Idealized TT-Nb_2O_5 Structure, Based on the T-Nb_2O_5 Unit Cell[a]

atom	position	o.f.	X	Y	Z
Nb (1)	4(h)	1.0	0.25	0.031 26	0.5
Nb (2)	4(h)	1.0	0.25	0.156 26	0.5
Nb (3)	4(h)	1.0	0.25	0.281 26	0.5
Nb(4)	4(h)	1.0	0.25	0.406 26	0.5

[a] See text for details on how these placements were obtained. X, Y, and Z coordinates are in fractions of the T-Nb_2O_5 unit-cell parameters along the a, b, and c axis, respectively; o.f. is occupancy factor.

We will now attempt to explain the structure of TT-Nb_2O_5 based on that of T-Nb_2O_5. A comparison of the two unit cells derived from XRD data indicates that they can be made to conform by judicious superimposition, as shown in Figure 3a, indicating that niobium atoms occupy equivalent positions in the two cells. The T-Nb_2O_5 unit cell contains 16.8 Nb atoms, the 16 major Nb positions illustrated in Figure 3b for T-Nb_2O_5 are in 8(*i*) positions. Each of these 32 Nb atom positions has an occupancy factor of 0.5, with the atom positions grouped in pairs, one slightly above and the other slightly below the indicated position in the *c* direction, with the average of each pair at $z = 0.5$. The remaining 0.8 Nb atoms are widely distributed in 4(*g*) type sites lying in the *a*–*b* plane at $z = 0$ with occupancy factors of less than 0.08 for a given position.[25] Comparison of TT- and T-Nb_2O_5 XRD results show that a single broad reflection in TT-Nb_2O_5 is split into two sharp reflections in T-Nb_2O_5 for the major spacings of TT-Nb_2O_5. The split reflections in T-Nb_2O_5 are probably due to this pairing of Nb atoms in the 8(*i*) positions. Assuming the TT-Nb_2O_5 structure is similar enough to T-Nb_2O_5 to allow the use of the same unit cell and basic atom positions, the split in X-ray reflections seen for T can be removed in TT by increasing the symmetry of the 8(*i*) positions to 4(*h*), reducing the number of Nb positions from 32 to 16, each now with an occupancy factor of 1.0, and reducing the number of possible reflections perpendicular to the appropriate plane in half. Thus, the Nb atoms in 4(*h*) positions in TT-Nb_2O_5 are distributed between the equivalent 8(*i*) positions of T-Nb_2O_5, on average being in the center, whereas in T-Nb_2O_5 they are fixed in either one or the other of the paired 8(*i*) positions. This difference would account for the broadening of X-ray diffraction peaks observed. In essence, TT-Nb_2O_5 can be considered as a disordering of the T-structure.

By removal of the 0.8 4(*g*) niobium positions in T-Nb_2O_5, the remaining Nb atoms can be relaxed into still more symmetric, evenly spaced positions, resulting in the Nb atom positions for TT-Nb_2O_5 listed in Table II. The removal of the 4(*g*) Nb atoms from T-Nb_2O_5 is justified when considering the fact that TT-Nb_2O_5 is less dense than T-Nb_2O_5,[15] about 4.93 vs 5.21 g/cm^3. Images calculated with the proposed TT-Nb_2O_5 structure are given in Figure 2 (shown on right); correspondence with the actual image is equally as good, if not better, as for the images simulated with the original T-Nb_2O_5 structure. An even better fit may have been obtained if the new oxygen positions could be determined, but there is no guide for the placing of oxygen, so the original positions given for oxygen in T-Nb_2O_5 were used.

The unit cell of T-Nb_2O_5 contains $Nb_{16.8}O_{42}$,[25] while the proposed cell for TT-Nb_2O_5, based on that of T-Nb_2O_5, now contains nonstoichiometric $Nb_{16}O_{42}$ with use of the above model. Obviously, not all of the oxygen positions can contain O. Several workers have reported that TT-Nb_2O_5 can exist only in the presence of stabilizing impurities such as OH^-, Cl^-, or F^- and is in fact a member of the homologous series $Nb_{6n-2}X_{16n-6}$, $n = 1, 2, 3, \ldots$, where X can be O, Cl, F, OH, etc.[13,15,16-18] Our work confirms this idea, in that in order for 16 Nb atoms to balance 42 oxygen positions, some of the oxygen positions must be replaced by monovalent ions or by oxygen-vacancy pairs, resulting in a formula of $Nb_{16}O_{38}Y_4$, where Y is OH, Cl, F, or (O + vacancy)$_{1/2}$. This allows for the intrinsic presence of "impurity" ions. To account for the differences in densities of TT- and T-Nb_2O_5, the possibility that Nb and balancing O or "Y" sites are also vacant cannot be ruled out. This model allows for the presence of OH groups in TT-Nb_2O_5. These may form intrinsically as a result of aqueous preparations or preparations yielding water as a byproduct. The presence of OH groups stabilizing TT-Nb_2O_5 has been previously alluded to.[8]

This model suggests that TT-Nb_2O_5 is orthorhombic, while it is believed to be monoclinic by X-ray work. Perhaps the "Y" atoms or Nb vacancies are ordered in such a way as to decrease the symmetry to that of monoclinic. Observations on single-crystal electron diffraction patterns of the "α"-Nb_2O_5 of Kosevich et al.,[31] identical with either TT- or T-Nb_2O_5, showed that the structure consists of domains of subcells within a superlattice. While the symmetry of the subcell is monoclinic, each domain can be ordered differently, resulting in orthorhombic symmetry for the superlattice. These differences in domain structures may be a result of vacancies or monovalent anion substitutions, as we have suggested. While this proposed structure of TT-Nb_2O_5, as given in Table II, needs further confirmation by single-crystal X-ray diffraction work, it serves as a guide to further investigation of this compound, and at the same time provides a framework for understanding previous experimental results on TT-Nb_2O_5. The two structures are similar and, as seen in Figure 2, difficult to tell apart. In the following discussion on thin films, the niobia form corresponding to TT- or T-Nb_2O_5 will be considered to be T-Nb_2O_5 for simplicity, although either or both may be occurring on the thin-film samples.

Model Thin Films. Thin films of niobia supported on silica were examined by HRTEM, and the results are given in Figures 4 and 5 together with corresponding simulated images. As *d* spacings determined experimentally by SADP for all our samples, including the four illustrated, matched the bulk values found by XRD, we assumed lattice spacings given for bulk niobia forms were valid for use in image calculations for thin-film crystals. Our original hope was to observe directly the transmission image of the film for the presence of crystallites or aggregates of niobia and then deduce the behavior and mechanisms responsible for their formation. While this method was suitable for low-resolution observations on larger sized crystals, imaging of small particles were extremely difficult due to interference from the comparatively thick silica film. To overcome this problem, a few images were taken at places where the film was either cracked or folded, allowing for clear observation of niobia particles projecting out over these edges. Sufficient observations were taken, both from edges and from the surface of the films, to ensure that the behavior of niobia observed on the edges was the same as that on other parts of the film. All of the images reproduced here are of particles near, or projected over, edges and can be considered representative of particles on the bulk silica surface.

As-deposited niobia thin films on silica are completely amorphous, and no additional contrast due to niobia is evident. Crystallized niobia on the heat-treated thin-film

(31) Kosevich, V. M.; Sokol, A. A.; D'yakonenko, Yu. P. *Sov. Phys. Cryst.* **1983**, *28*, 285.

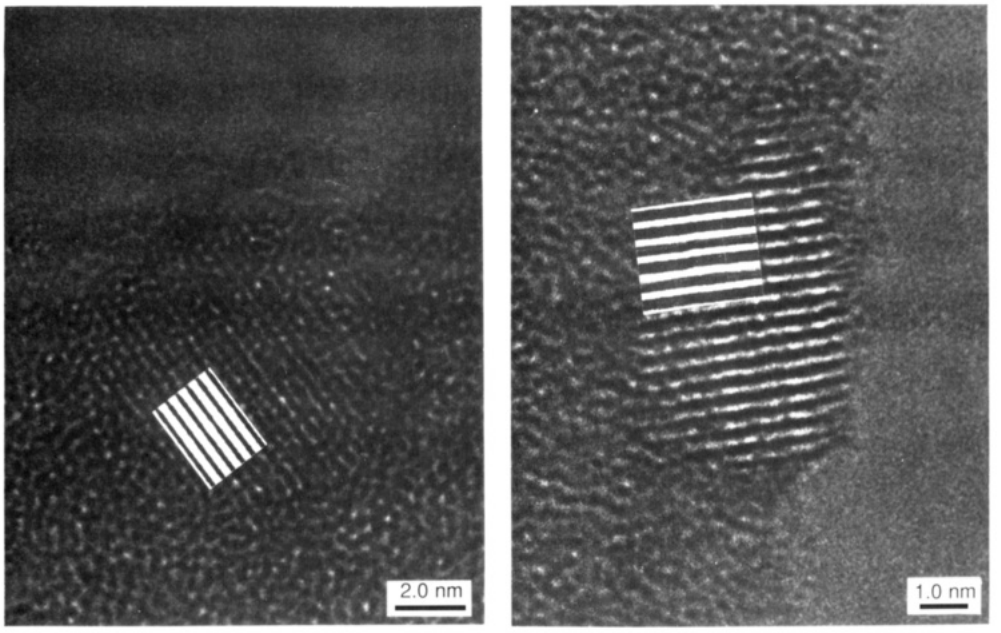

Figure 4. HRTEM and image simulation of T-Nb_2O_5 crystals on model thin films. (a) T-Nb_2O_5 (100) on 12(873,16). Image simulated at slice 9- and 18.5-Å thickness, −460-Å defocus. (b) T-$Nb_2O_5(2\bar{1}0)$ on 4(873,16). Image simulated at slice 5- and 9.5-Å thickness, −200-Å defocus.

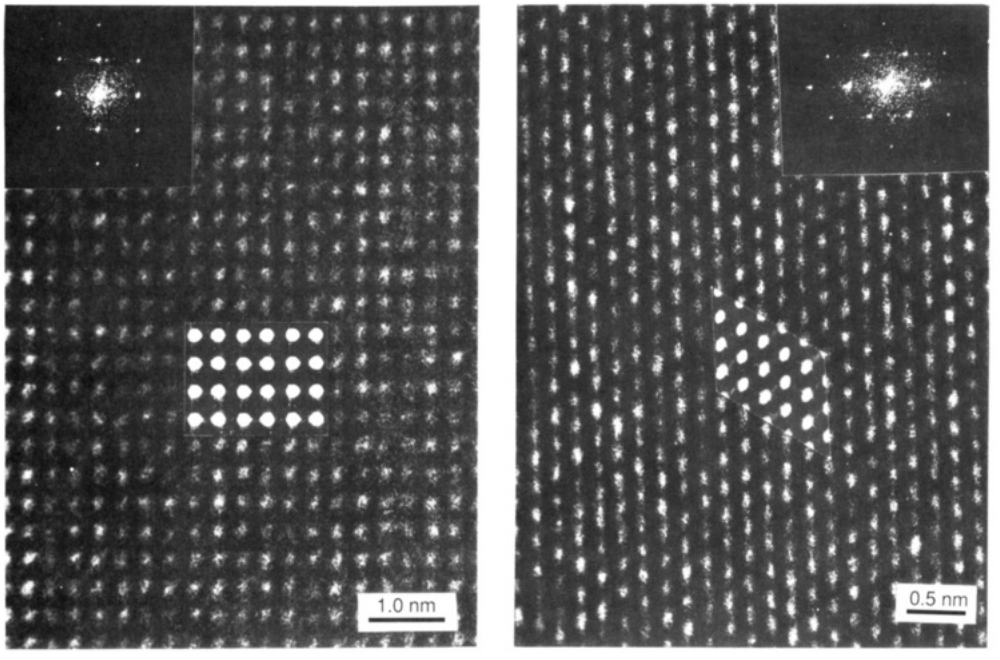

Figure 5. HRTEM and image simulation of H-Nb_2O_5 crystals on model thin films. (a) H-Nb_2O_5(203) crystal on 50(873,2) and corresponding optical diffraction pattern, correctly oriented. Image simulated at slice 10- and 20-Å thickness, −600-Å defocus. (b) H-$Nb_2O_5(6\bar{3}1)$ crystal on 50(873,2) and corresponding optical diffraction pattern, correctly oriented. Image simulated at slice 25- and 50-Å thickness, 0 defocus.

samples can be roughly grouped by size into two categories. The smallest crystals, having an average diameter of less than 100 Å, produced images almost without exception consisting of parallel lattice fringes of about 3.9-Å spacing. Examples are given in Figure 4. The larger crystals, over 500 Å in diameter, have well-defined lattice fringes repeating uniformly throughout the crystal, as illustrated in Figure 5.

The smallest crystals were identified as T-Nb_2O_5 on the basis of their 3.9-Å spacing, corresponding to the distance between rows of niobium atoms in the T-Nb_2O_5 unit cell, looking down the *c* axis, as indicated in Figure 3b. These small crystals correspond to the type II niobia mentioned in the Introduction. The simplest orientation would correspond to (100), although conceivably the unit cell could be tilted considerably around either or both the *a* or *b* axis while still maintaining the predominant rows of Nb atoms spaced 3.9 Å apart. Because the Nb atoms are so aligned, there are no possibilities for the generation of cross-fringes in the lattice images, as a consequence many orientations of the form (*hk*0) yield essentially the same image: parallel fringes spaced 3.9 Å apart. Examples of

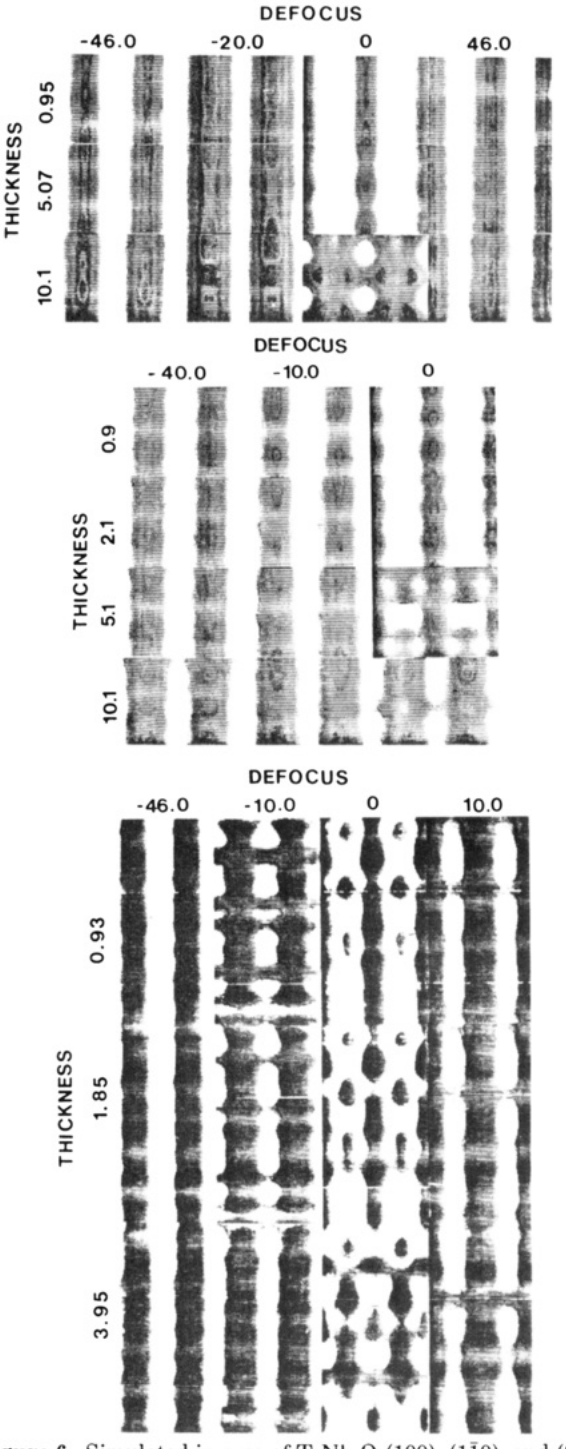

Figure 6. Simulated images of T-Nb_2O_5(100), (1$\bar{1}$0), and (2$\bar{1}$0) for a range of thickness and defocus conditions. Although crystal orientation and simulation parameters can be modified over a range of conditions, the images simulated are all similar except at conditions where phase-contrast reversals take place. Comparison of these simulations with actual T-Nb_2O_5 images, as in Figure 4, show that most of the simulated images illustrated here could equally match the actual images, indicating that there is significant uncertainty in assigning thickness, defocus, and orientation to actual T-Nb_2O_5 images, although the identity of the form is certain. Orientations are (top) (100), (middle) (1$\bar{1}$0), and (bottom) (2$\bar{1}$0).

this behavior are calculated in Figure 6. Similar images, but with either wider or narrower fringes, were obtained at greater or smaller values of defocus. Image calculations of other niobia forms did not produce parallel lattice fringes of the correct spacing. Although there are changes in relative width of the fringes, nearly any of the calculated images in Figure 6 could have matched the actual images of Figure 4. Only in cases where phase contrast reversals occur in the calculated images, as in T-Nb_2O_5 at 9.3- and 18.5-Å thickness and −100-Å defocus for (100), 51-Å thickness and 0 defocus for (1$\bar{1}$0), and so on, is this not true. However, imaging these small particles proved to be difficult, and no crystals were observed at a defocus where these additional contrast features appeared.

The small variations in fine details seen in the simulated images of Figure 6 are easily negated by interference in the actural images due to the underlying amorphous silica thin film, making comparison between actual and calculated T-Nb_2O_5 images of this type impossible. While the identity of the crystals is assuredly T-Nb_2O_5 (or TT-Nb_2O_5), the specific orientation and thickness of the actual crystals cannot be determined with any degree of reliability. Only two instances occurred where other orientations among the small-sized crystals were noted. These were successfully simulated as T-Nb_2O_5(001) and T-Nb_2O_5(101).[10]

Images of the large crystals were much easier to simulate than those of T-Nb_2O_5. In all cases these were H-Nb_2O_5. Corresponding simulated images are given in Figure 5a for H-Nb_2O_5(203) and in Figure 5b for H-Nb_2O_5(6$\bar{3}$1). The slight differences in appearance between the simulated and calculated images are most likely due to small crystal or beam tilt. Both of these figures are for 50(873,2) samples. H-Nb_2O_5 was found to occur also on 4(873,16) and 12(873,6) samples, in all cases as type III niobia, crystallizing without restraint from the substrate. The optical diffraction patterns for these two figures could not be indexed satisfactorily to other niobia forms, further confirming our assignment of H-Nb_2O_5.

Niobia Phase Stability. The pathway to more stable niobia forms depends on a variety of factors including preparation method, impurities, and rate and temperature of heating.[12] TT-Nb_2O_5 appears kinetically first as the coordination of niobium with oxygen in the amorphous precursors is closer to 7-fold, so there is little barrier to TT-Nb_2O_5 formation. No thermal effect is found in the transformation from TT- to T-Nb_2O_5, as no major rearrangement of atoms is necessary.[13,16,18] We thus consider the two forms (TT and T) to be similar an energy. On the other hand, there must be a considerable activation energy barrier in the transformation to the more stable niobia forms, as temperatures of over 1073 K and/or long heating times have been noted to effect transformations such as T → M or T → B.[15,16] Additional heating is needed to convert B- and M- into H-Nb_2O_5. These observations are summarized qualitatively by curve a in Figure 7, where relative free energies of the various niobia forms are plotted against the order of crystallization. The main reason for this behavior is that the coordination of oxygen to niobium in TT- and T-Nb_2O_5 is 7-fold, while the coordination is octahedral, 6-fold, in M-, N-, B-, and H-Nb_2O_5.

In the literature B-Nb_2O_5 is thought to be the stable form of niobia below about 1023 K, but there is some evidence that H-Nb_2O_5 is the only stable niobia form at atmospheric pressures.[15,20] We now have conclusive evidence from this work that H-Nb_2O_5 can form at temperatures as low as 873 K. H-Nb_2O_5 in our samples crystallized in conjunction with T- (or TT-) Nb_2O_5, although by different mechanisms. The behavior of our samples is illustrated by curve b in Figure 7. The as-deposited niobia, while amorphous, could occur in two ways, destined to become types I, II, and III, as described in the Introduction. Type I remains amorphous, being strongly held to the surface; some niobia, starting at point 1 on curve b,

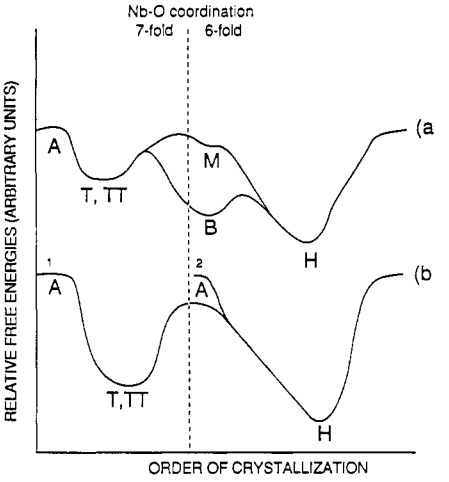

Figure 7. Relative free energies of niobia forms from previous works and this work. Diagram indicates the qualitative changes in energies as niobia crystallization proceeds from amorphous niobia, starting at points 1 from chemical deposition or 2 from physical deposition on the left, to the stable form, H-Nb_2O_5, on the right. Curve a is based on ref 12, 13, 15–17, 20, and 22. Curve b is based on this work.

has a higher coordination with oxygen and so forms T-Nb_2O_5, type II. Type II may be influenced by type I surface-oxide niobia and is mostly stabilized against further changes.[8,10,32] Other as-deposited niobia may have a lower, 6-fold, coordination of niobium with oxygen due to the physical deposition method used and so is able to proceed directly to H-Nb_2O_5 upon heat treatment.

While none of the samples heated to less than 873 K in this work examined by HRTEM contained H-Nb_2O_5, there is evidence from conventional TEM observtions that for longer heating times, at least 16 h, H-Nb_2O_5 may form at temperatures as low as 773 K.[10] The majority of niobia in our samples is H-Nb_2O_5, the presence of metastable T-Nb_2O_5 being explained by the effects of the silica support on some of the niobia. No evidence for other stable forms was found, so we conclude that H-Nb_2O_5 is the stable form under the conditions studied. Perhaps the reason for the differences between this and previous work lies in the nature of the niobium precursors used. While previous workers prepared niobia from niobic acid, NbO_2, or niobium oxychlorides, we used reactive radio-frequency deposition. The different preparation techniques, chemical versus physical, undoubtedly resulted in different amorphous structures and consequently different behavior toward heat treatment.

Conclusions

This work has shown the usefulness of HRTEM in determining ambiguous crystalline structures and their relationship to thermal treatment. Perhaps just as important, we have shown that HRTEM is not always definitive and, in certain cases, can yield only limited information on particular phases. This point is illustrated by the indistinguishability of TT/T-Nb_2O_5 in our thin-film samples and the inability to determine the orientation, defocus, or thickness of TT or T crystals in these samples.

We have shown that the structure of TT-Nb_2O_5 is nearly identical with that of T-Nb_2O_5. A structure having the same unit cell but simpler atom positions is proposed for TT. This structure may contain monovalent anions as well as the possibility of vacancies in both the niobium and anion positions and may be described by the unit-cell formula of $Nb_{16}O_{38}Y_4$, where Y is OH, Cl, F, or $(O + \text{vacancy})_{1/2}$. Observations of dissimilarities between the two structures in this and other work are attributed to these chemical differences. Furthermore, the main difference between the two forms may lie in the presence of OH groups in TT-Nb_2O_5.

We found the presence of small T- (or TT-) Nb_2O_5 and large H-Nb_2O_5 crystals in the thin-film samples. These observations were confirmed by image simulation. As noted earlier, the similarity of the TT- and T-Nb_2O_5 structures made the two forms indistinguishable in HRTEM. The observation of H-Nb_2O_5 as the predominant phase formed at 873 K in our samples suggests that it is the only stable form of niobia at atmospheric pressures and all temperatures below about 1700 K.

Finally, these results illustrate the applicability of HRTEM imaging and image simulation to obtaining important structural information on model thin films. A comparison between these films and their high-surface-area counterparts[8] allows an understanding of the stability of various structures toward heat treatments (such as calcining) in terms of interfacial interactions between the deposited and the supporting oxides. Since these interactions can to some extent be controlled by the preparative method, such knowledge is important in establishing a link between the microstructure of a catalyst and its chemical behavior.

Acknowledgment. This work was supported by the Center for Study of Materials at Carnegie Mellon University (CMU) under Grant DMR-8521805 and by the Niobium Products Co., Inc. High-resolution electron microscopy was supported by the Center for High Resolution Electron Microscopy in the Center for Solid State Science at Arizona State University (ASU), established with support from NSF under Grant DMR-8306501. We thank John Barry at ASU for operating the JEOL 4000EX, Rodger Graham at ASU for arranging for the use of their facilities, and Peter Burke at CMU for preparing the pure niobia phases.

Registry No. Nb_2O_5, 1313-96-8; Nb, 7440-03-1.

(32) Burke, P. A.; Weissman, J. G.; Ko, E I.; Wynblatt, P. *Catalysis 1987*; Ward, J. W., Ed.; Elsevier: Amsterdam, 1988; p 457.